TURBULENT FLOW OVER CARS

A. R. Azimian

Department of Mechanical Engineering
Isfahan University of Technology
Isfahan, Iran

Abstract In this paper the flow behaviour over a number of car bodies is studied. For this purpose the unsteady 2-D incompressible Navier-Stokes equations have been applied. After averaging and nondimensionalizing the equations, the system of equations has been transformed from the Cartesian (x-y) coordinates to a body fitted generalized (ξ-η) coordinate. As the flow is incompressible, the density in the continuity equation will disappear and thus the coupling between the continuity and the momentum equations will be lost. To resume the missing coupling between the aforementioned equations an artificial state equation is introduced. This artificial state equation will couple the continuity and the momentum equations via pressure. For turbulence simulation Jones & Launder's Low Reynolds turbulence model was employed. By means of an implicit method, the system of five equations are solved. From the flow field solution, the drag force on car geometries are predicted and the results are compared to the drag force calculated from experimental correlations. Agreement is fare enough i.e. within 90 percent of accuracy.

Key Words Turbulent Flow, Car Bodies, Navier-stokes Equations, Drag Force, Artificial State Equation

چکیده در این مقاله سعی شده است تا رفتار جریان هوا را بر روی بدنه تعدادی خودرو بررسی نماییم. برای این منظور معادلات ناویر-استوکس دوبعدی غیر دائم را به کار برده ایم. پس از متوسط گیری و بی بعدسازی معادلات، آنها را از دستگاه مختصات دکارتی (x-y) به دستگاه مختصات منطبق بر بدنه (ξ-η) منتقل کرده ایم. از آنجا که سیال تراکم‌ناپذیر است، چگالی در معادله پیوستگی ظاهر نمی شود و در نتیجه ارتباط بین معادلهٔ پیوستگی و ممنتم از بین می‌رود. برای ایجاد ارتباط بین این معادلات از یک معادلهٔ حالت مصنوعی استفاده می شود که معادلات پیوستگی و ممنتم را از طریق فشار به هم مربوط می کند. برای مدل کردن اغتشاش از مدل جونزو لاندر بارینولدز پائین استفاده می کنیم و دستگاه معادلات پنجگانه حاصل را به روش ضمنی حل می کنیم. از روی نتایج میدان جریان بر روی بدنهٔ خودروها نیروی درگ را محاسبه کرده و با نیروی درگ بدست آمده از روشهای تجربی مقایسه می کنیم که توافق حدود ۹۰٪ را نشان می دهد.

INTRODUCTION

Prediction of the drag force on car geometries are of prime importance for designers of this sort of shapes. The air drag force on a car geometry is usually calculated from the pressure and velocity field around the body. Wind tunnels are normally used to measure the pressure and velocity around a model or possibly a full scale car geometry. From the measured results, it is possible to make some correlations which could be used to predict the drag force (for example see the results of Reference 1. However, the experimental tests are both time consuming and expensive. Therefore, if we can model the flow behaviour around a car shape numerically, it would be possible to predict the drag force from the calculated pessure and velocity field, which will save time and money. Solution of the flow field around simple geometries are reported by many researchers such as Lin [2], Selika [3] and Payne [4]. However from these simple bodies results it is not possible to make any conclusion on complicated car geometries. On the other hand the flow analysis around the car bodies are classified by car makers and therefore the published materials in this regard are rare. In the present work it is attempted to model the flow behaviour on a number of car

shapes. To simplify the problem, the flow under the car body and the effect of car wheels are ignored. In order to assess the performance of the program the following steps were taken: First, the drag coefficients of two selected car geometries are extracted from the wind tunnel results of Reference 1 and these results are compared i.e. their ratio are calculated. Second, for the simplified shapes of the aforementioned car bodies the program is run and the predicted drag coefficients are compared. Third, the ratio of the predicted drag coefficients are compared to the ratio of the drag coefficient which was calculated based on wind tunnel correlation. Comparison of the two sets of results for the tested cases appeared to be promissing.

GOVERNING EQUATIONS

The unsteady 2-D incompressible Navier-Stokes equations are the governing equations which are as follow:

$$\partial u/\partial x + \partial v/\partial y = 0 \qquad (1)$$

$$\partial(\rho u)/\partial t + \partial(\rho u^2 + p - \tau_{xx})/\partial x + \partial(\rho vu - \tau_{yx})/\partial y = \rho f_x \qquad (2)$$

$$\partial(\rho v)/\partial t + \partial(\rho vu - \tau_{yx})/\partial x + \partial(\rho v^2 + p - \tau_{yy})/\partial y = \rho f_y \qquad (3)$$

where

$$\tau_{xx} = \lambda \nabla.\vec{v} + 2\mu \partial u/\partial x \quad , \quad \tau_{yy} = \lambda \nabla.\vec{v} + 2\mu \partial v/\partial y \qquad (4)$$

$$\tau_{yx} = \tau_{xy} = \mu(\partial v/\partial x + \partial u/\partial y), \quad , \quad \lambda = -2/3\mu$$

where μ is the dynamic viscosity coefficient and λ is the bulk viscosity coefficient. It is worth noting that in Equations 2 and 3 the friction forces (f_x, f_y) are considered to be zero. The aforementined equations could be nondemensionalized by means of the following reference parameters:

$$u^+ = u/u_\infty \quad , \quad v^+ = v/u_\infty \quad , \quad x^+ = x/L_{ref} \quad , \quad y^+ = y/L_{ref}$$

$$\rho^+ = \rho/\rho_{ref} \quad , \quad \mu^+ = \mu/\mu_{ref} \quad , \quad t^+ = t.u_\infty/L_{ref}$$

$$p^+ = p/\rho_{ref}.u^2_\infty \quad , \quad Re_\infty = \rho.u_\infty.L_{ref}/\mu$$

Where u_∞ is freestream velocity which for this study was the air velocity of 16.6 m/s, corresponding to a car velocity of 60.0 Km/h. Also p_{ref}, ρ_{ref}, and μ_{ref} are pressure and air properties at freestream conditions. The characteristic length or reference length (L_{ref}) is the car length. After nondimensionalizing the governing equations are as follow:

$$\partial u/\partial x + \partial v/\partial y = 0 \qquad (5)$$

$$\partial u/\partial t + u.\partial u/\partial x + v.\partial u/\partial y = -\partial p/\partial x + 1/Re_\infty(\partial^2 u/\partial x^2 + \partial^2 u/\partial y^2) \qquad (6)$$

$$\partial v/\partial t + u.\partial v/\partial x + v.\partial v/\partial y = -\partial p/\partial y + 1/Re_\infty(\partial^2 v/\partial x^2 + \partial^2 v/\partial y^2) \qquad (7)$$

ARTIFICIAL COMPRESSIBILITY

In the equations presented above u, v, and p are unknowns. The pressure does not appear in the continuity equation and hence the coupling between these equations with respect to the pressure is lost. There are many ways to overcome this problem. The SIMPLE algorithm used by Patankar [5] is a famous one. Integrating **u** momentum equation with respect to **y** and **v** momentum equation with respect to **x**, and subtracting the two equations, the pressure term will cancel out from the momentum equations. The resulting equation combined with the continuity

equation will end up with a Poisson type equation [6] which, upon the solution, will provide the velocity field. This is a good procedure for steady 2-D problems, but due to the errors generated in mass balance [7] it is set aside. The method proposed by Chorin [8] uses an artificial state equation, as following:

$$p = \kappa\rho \tag{8}$$

where **p** is the pressure, ρ is the density and $\kappa > 0$ is the artificial compressibility factor. By using the above equation the unsteady continuity equation becomes:

$$\partial p/\partial t + \kappa(\partial u/\partial x + \partial v/\partial y) = 0 \tag{9}$$

The value of the κ should be selected in such a way that the system of equations reach the steady state as fast as possible. Its value is selected by trial and error.

GENERALIZED COORDINATE

Car bodies have complicated geometry and cartesian coordinate is only suitable for simple rectangular shapes. Therefore, it is necessary to transfer the governing equations from (x-y) coordinate to a body fitted general (ξ-η) coordinate. The resulting transformed equations are,

$$\partial p/\partial t + \kappa[y_\eta \partial u/\partial\xi - y_\xi \partial u/\partial\eta + x_\xi \partial v/\partial\eta - x_\eta \partial v/\partial\xi]1/J = 0 \tag{10}$$

$$\partial u/\partial t + [y_\eta \partial^2 u/\partial\xi^2 - y_\xi \partial^2 u/\partial\eta^2]1/J + [x_\xi \partial uv/\partial\eta - x_\eta \partial uv/\partial\xi]1/J - (\sigma\partial u/\partial\eta + \tau\partial u/\partial\xi]1/Re_\infty J^2 + [y_\eta \partial p/\partial\xi - y_\xi \partial p/\partial\eta]1/J = [\alpha\partial^2 u/\partial\xi^2 - 2\beta\partial^2 u/\partial\xi\partial\eta + \gamma\partial^2 u/\partial\eta^2]1/Re_\infty J^2 \tag{11}$$

$$\partial v/\partial t + [x_\xi \partial^2 v/\partial\eta^2 - x_\eta \partial^2 v/\partial\xi^2]1/J + [y_\eta \partial uv/\partial\xi - x_\xi \partial uv/\partial\eta]1/J - (\sigma\partial v/\partial\eta + \tau\partial v/\partial\xi]1/Re_\infty J^2 + [x_\xi \partial p/\partial\eta - x_\eta \partial p/\partial\xi]1/J = [\alpha\partial^2 v/\partial\xi^2 - 2\beta\partial^2 v/\partial\xi\partial\eta + \gamma\partial^2 v/\partial\eta^2]1/Re_\infty J^2 \tag{12}$$

where the parameters are:

$$x_\xi = \partial x/\partial\xi \ , \ x_\eta = \partial x/\partial\eta \ , \ y_\xi = \partial y/\partial\xi \ , \ y_\eta = \partial y/\partial\eta \ ,$$

$$J = x_\xi y_\eta - x_\eta y_\xi \ , \ \alpha = x^2{}_\eta + y^2{}_\eta \ , \ \beta = x_\xi x_\eta + y_x y_\eta \ ,$$

$$\gamma = y^2{}_\xi + y^2{}_\xi \ , \ \sigma = (y_\xi D_x - x_\xi D_x)/J, \ \tau = (x_\eta D_y - y_\eta D_x)/J,$$

$$D_x = \alpha x_{\xi\xi} - 2\beta y_{\eta\eta} + \gamma x_{\eta\eta} \ , \ D_y = \alpha y_{\xi\xi} - 2\beta y_{\xi\eta} + \gamma y_{\eta\eta} \tag{13}$$

TURBULENCE MODEL

By taking into account the overall size of a car body and the kinematic viscosity of the air which is the working fluid, the Reynolds number would be high enough to consider the flow as a turbulent flow. To model the turbulence, the two-equation K-ε model of Jones and Launder [9] is used in this study. Michelassi and Shih [10] have shown that in the flows with high adverse pressure gradients the high Reynolds number version of Jones and Launder model does not provide accurate results. Therefore, a low Reynolds version of their model which is accurate enough near the walls is used so that there is no need to consider wall function. **K equation** (rate of kinetic energy generation)

$$\rho DK/Dt = \partial[(\mu+\mu_T/\sigma_k)]/\partial y + \mu_t (\partial u/\partial y)^2 - \rho\varepsilon - 2\mu [\partial k^{0.5}/\partial y]^2 \tag{14}$$

ε equation (rate of kinetic energy dissipation)

$$\rho D\varepsilon/Dt = \partial[(\mu + \mu_T/\sigma_\varepsilon)\partial\varepsilon/\partial y]\partial y + c_1 f_1 \varepsilon/K \mu_T [\partial u/\partial y]^2 - c_2 f_2 \rho\varepsilon^2/K + 2\mu\mu_T/\rho \ [\partial^2 u/\partial y^2]^2 \tag{15}$$

where

$$\mu_T = c_\mu f_\mu \rho K^2/\varepsilon \ , \ K_T = c_p \mu_T/0.9 \tag{16}$$

and the constants are,

$c_\mu = 0.09$, $c_1 = 1.55$, $c_2 = 2$, $\sigma_k = 1$, $\sigma_\varepsilon = 1.3$

and for **f** constants one has

$f_1 = 1$, $f_2 = 1.0 - .3\exp(-R^2)$, $f_\mu = \exp[-2.5/(1+R/50)]$

where $R = \rho k^2/\mu\varepsilon$ is the turbulence Reynolds number.

COMPUTER MODELING AND SOLUTION ALGORITHM

As the Navier-Stokes equations are nonlinear, they are linearized. Further, all the space derivatives that appear in Equations 10, 11, and 12 are discretized with second order accurate central finit differences. After linearization and rearangement of the equations a tridiagonal system of equations for **u, v** and **p** is obtained. By means of an alternating direction implicit technique (ADI) this tridiagonal system of equation is solved. Using the results of this system of equations the **K** and ε equations are solved separetly. Therefore, the mass and momentum equations are not coupled to the **K** and ε equations. To start the solution procedure a guess of the initial conditions is required. The free stream condition is a good initial guess to start with. The solution will continue until the steady state is reached which is the final answer.

BOUNDARY CONDITIONS

A set of boundary conditions have to be defined which are chosen as follows:

1) Inlet (Left): At the inlet a given velocity profile is imposed. The pressure is computed imposing its second order derivative in the direction of the flow equal to zero which becomes as following:

$$\partial^2 p/\partial x^2 = 0 \quad , \quad u = u(y) \quad , \quad v = 0 \qquad (17)$$

2) Outlet (Right): At the outlet the parallel flow condition is assumed. Such a condition implies that the eventual disturbances introduced in the domain are now completely damped so that, at the downstream boundary, the flow pattern will not change any more.

$$\partial u/\partial x = 0 \quad , \quad \partial v/\partial x = 0 \quad , \quad v = 0 \qquad (18)$$

3) Solid Wall (Lower): At the solid wall the no slip condition is applied, therefore the velocity components are both set to zero. The pressure at the wall is computed with the momentum equation normal to the wall obtained by a suitable linear combination of the momentum equations in the two coordinate directions, i.e.

$$\partial p/\partial n = 1/Re\ \partial^2 u_n/\partial n^2 \quad , \quad u = 0 \quad , \quad v = 0 \qquad (19)$$

4) Far Field (Upper): The upper boundary is set far enough from the body in such a way that there would be no influence of the body on it.

$$u = u_\infty, \quad v = 0, \quad \partial\phi/\partial y = 0 \qquad (20)$$

Where ϕ can be any variable.

GRID GENERATION

The choice of the cartesian orthogonal coordinate leads to the standard form of the Navier-Stokes equations with a simple rectangular mesh system. Nevertheless, the lack of generality of a code based on this option becomes evident as soon as it becomes necessary to deal with a physical domain in which the boundaries are not aligned with the coordinate axes. A curvilinear non-orthogonal coordinate mesh was chosen, where the boundaries of any flowfield can be made to coinside with coordinate lines. Several ways to produce such a domain are available, ranging from algebraic transformations to the solution of elliptic partial differential equations with a smoothly

generated mesh [6]. The method of Thompson [11] is used in the present work, where the following Laplace equations could be solved.

$$\nabla^2\xi = 0 \quad , \quad \nabla^2\eta = 0 \tag{21}$$

where ξ and η are the coordinates in the computational domain. In order to cluster points in regions with high gradients, the exponential weighting functions, $p(\xi,\eta)$ and $q(\xi,\eta)$ are introduced, and the Poisson equations are solved.

$$\nabla^2\xi = p(\xi,\eta) \quad , \quad \nabla^2\eta = q(\xi,\eta) \tag{22}$$

Where $p(\xi,\eta)$ and $q(\xi,\eta)$ are as follows:

$$p(\xi,\eta) = -\sum_{i=1}^{m} a_i \, \mathrm{sgn}(\xi - \xi_i) \exp(-c_i|\xi - \xi_i|)$$

$$-\sum_{j=1}^{n} b_j \mathrm{sgn}(\xi - \xi_j) \exp\left(-d_j\sqrt{(\xi-\xi_j)^2+(\eta-\eta_j)^2}\right) \tag{23}$$

$$q(\xi,\eta) = -\sum_{i=1}^{m} a_i \, \mathrm{sgn}(\eta - \eta_i) \exp(-c_i|\eta - \eta_i|)$$

$$-\sum_{j=1}^{n} b_j \mathrm{sgn}(\eta - \eta_i) \exp\left(-d_j\sqrt{(\xi-\xi_j)^2+(\eta-\eta_j)^2}\right) \tag{24}$$

Where **m** is the number of constant grid lines ξ and/or η in which clustering is enforced, whereas ξ_i and η_i specify the lines. Similarly **n** is the number of grid points arround which clustering is enforced with ξ_j and η_j specifying the points. Also **a** and **b** are amplification factors and **c** and **d** are decay factors respectively. Proper values of these constants are selected by trial and error. The first term in Equation 23 has the effect of attracting the ξ= constant lines to $\xi = \xi_i$ and the second term causes ξ= constant lines to be attracted to the points (ξ_j,η_j). In Equation 24 similar effect on η= constant lines happen. The use of the sign-changing (sgn) function is only necessary to cause attraction to both sides of a line or point in the field. The (sgn) was defined as sgn(x) to be 1, 0, or -1 depending on whether **x** is positive, zero, or negative.

COMPUTER PROGRAM

To carry on the calculation a computer program written in Fortran 77 was used. In order to check the generality and accuracy of the program, first the flow over a step was solved, and its results are shown in Figure 1 which qualitatively agrees well with the results published by Michelassi and Benocci [7]. Figure 1a shows the generated mesh while Figures 1b and 1c show the velocity vectors and streamlines respectively. The effect of the number of mesh points on the accuracy of the results was assessed and it was found that as the number of grid points are increased the mass error is decreased (see Table 1). However, the final grid points are 66*26 which is close to the capabality limit of the computer used, i.e. DX2-486.

TABLE 1. The Results of a Grid Study.

Number of Grid Points	Mass Error %
16 * 10	0.011350
25 * 16	0.007471
55 * 31	0.002019

RESULTS

Two car bodies were selected, i.e. Citroen-2CV and Renault-5. The results published by Reference 1 indicate that the drag coefficient for these cars are 0.52 and 0.42 respectively. The ratio of the drag coefficients for these two cases is 1.23. Then the program was run for the aforementioned car bodies and the ratio of the drag coefficients was found to be 1.1 which is in good agreement with the test results and the difference is about 12 percent which is

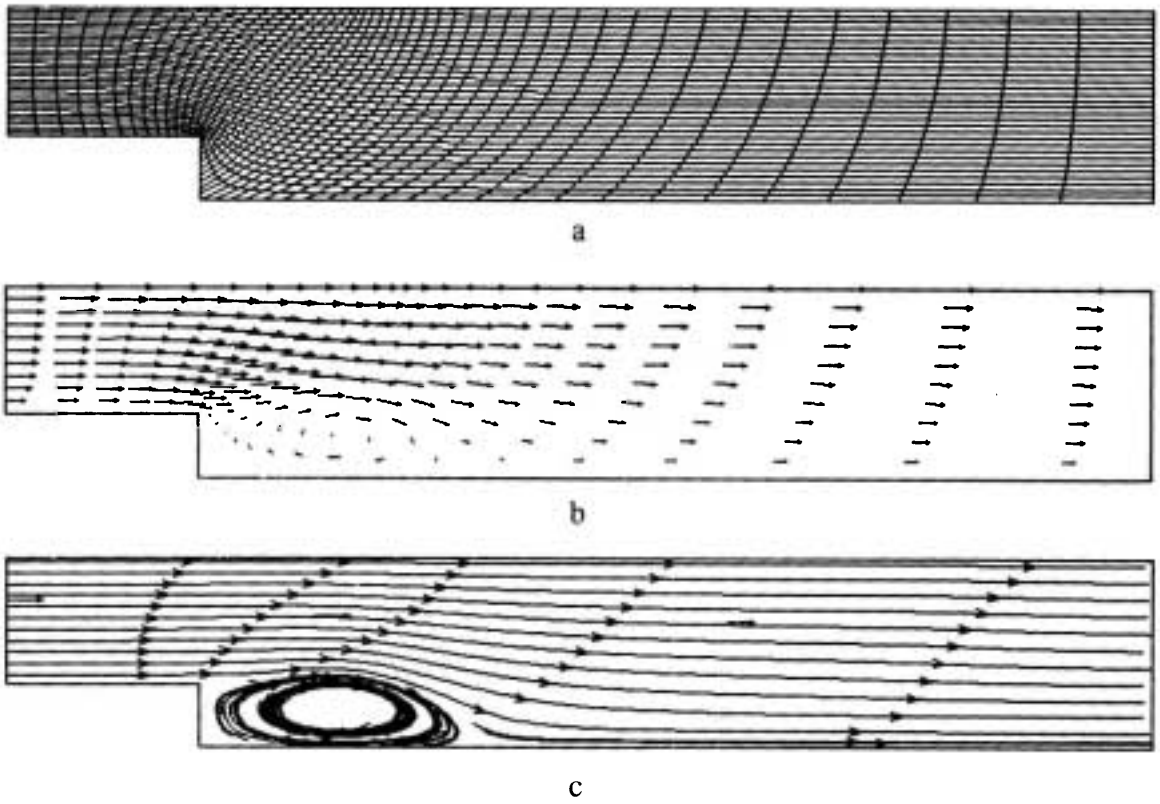

Figure 1. a) Body fitted mesh for a step. **b)** Vector plots for flow over a step. **c)** Streamlines for flow over a step.

considered to be reasonable. Figures 2a and 3a show the generated grids for the Citroen-2CV and Renault-5, respectively. In Figures 2b and 3b the velocity vector plots for both bodies are shown. The streamlines of the aforementioned cars are shown in Figures 2c and 3c. As it is shown in Figures 2d and 3d the reciculating flow behind the cars are quite clear and it is more pronounced for Citroen-2CV. Therefore, the predicted drag coefficient for this car is greater than Renault-5. Moreover, another car known as (Paykan) was tested. The generated mesh, velocity vectors and streamlines for this geometry are shown in Figures 4a, 4b and 4c respectively. Again the recirculating flow for this car is shown in Figure 4d. The size of this recirculating flow in comparison to the other two cars is smaller. Hence, it is expected to have smaller drag coefficient, for this car. To calculate the drag coefficient, the correlation introduced in Reference 1 is used which is as follows;

$$C_D = 0.16 + 0.0095R_T$$

Where R_T is a constant of which its value depends on configurations used in front, rear, sides, roof, etc., of a car geometry. The values of R_T can be extracted from the information supplied in tables of Reference 1. However, using the information obtained from Reference 1, the drag coefficient of Paykan geometry was calculated and compared to that of Citroen 2-CV. The ratio of the calculated drag coefficient for this car with respect to the Citroen-2CV was found to be 0.85. Therefore, using this value and the value of 0.52 which is the drag coefficient of the Citroen-2CV, the predicted drag coefficient for the Paykan would be 0.44. Now, if we use the correlations of Reference 1, the predicted drag coefficient for the Paykan body

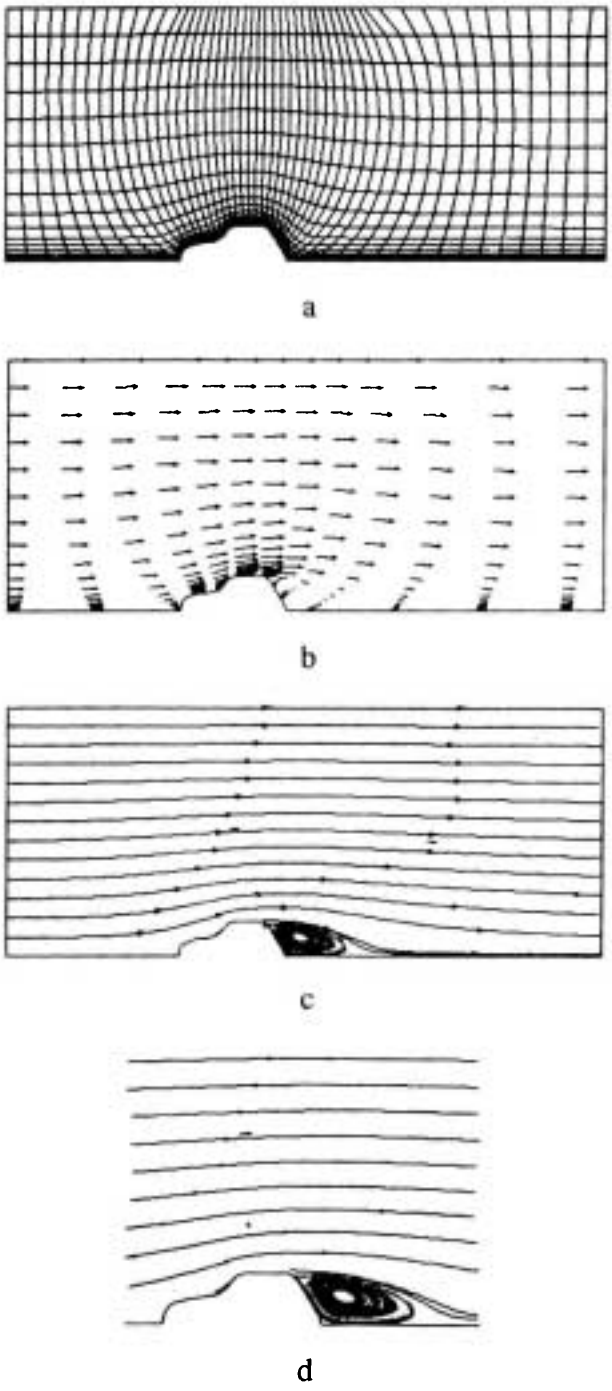

Figure 2. a) Body fitted mesh for a Citroen-2CV car. **b)** Vector plots for flow over a Citroen-2CV car ($Re_\infty = 5\times10^6$). **c)** Streamlines for flow over a Citroen-2CV car ($Re_\infty = 5\times10^6$). **d)** Vortex behind the Citroen-2CV car.

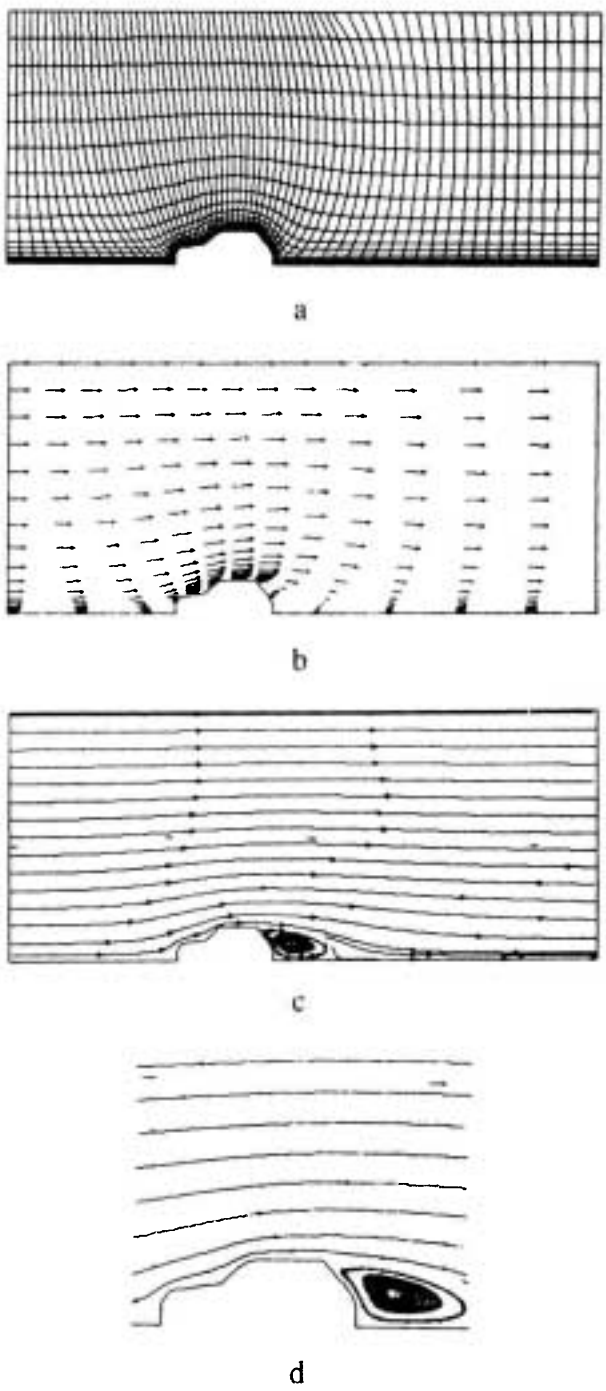

Figure 3. a) Body fitted mesh for a Renault-5 car. **b)** Vector plots for flow over a Renault-5 car ($Re_\infty = 5\times10^6$). **c)** Streamlines for flow over a Renault-5 car ($Re_\infty = 5\times10^6$). **d)** Vortex at the rear of a Renault-5 car.

would be 0.46. Comparison of the two values shows only a small difference. Examination of the aforementioned test cases reveal that it is possible to run the program for any car body of interest and predict the drag coefficient within about 90 percent of accuracy. Also, it is possible to perform any change

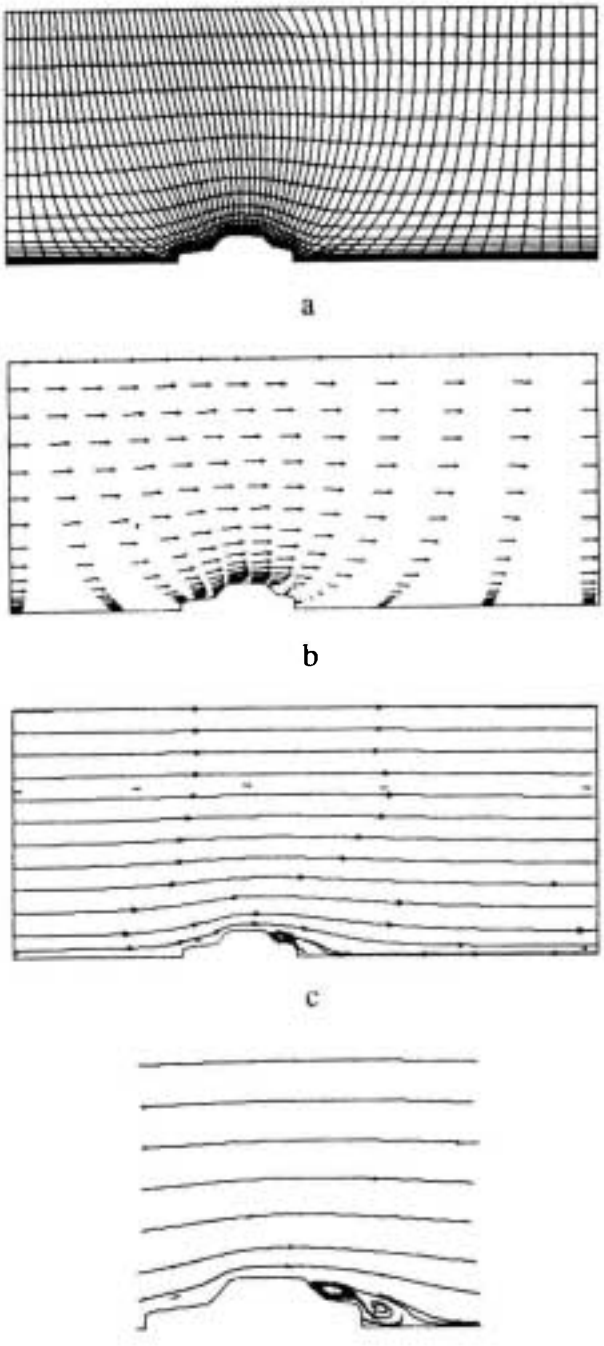

Figure 4. a) Body fitted mesh for a Paykan car. **b)** Vector plots for flow over a Paykan car ($Re_\infty = 5\times10^6$). **c)** Streamlines for flow over a Paykan car ($Re_\infty = 5\times10^6$). **d)** Vortex behind the Paykan body.

in an existing car geometry and examine the effect of the possible changes on the drag coefficient. Obviously, if any drag reduction could be observed from a possible modification, from drag coefficient estimation it is possible to calculate the power saving and also reduction in the fuel consumption. By predicting any amount of fuel to be saved it would be possible to calculate its impact on the reduction of air pollution which is another important matter. Moreover, it is worth to emphesize the impact of the application of the results of this type of study on car making industry. It is possible to apply the results of this type of work on geometry optimization of their products. From any optimization obtained in this way it would be possible to have some savings on sheet metal work as well. Furthermore, it is worth noting that the experimental results which were refered to in this paper are for 3-D car geometries. The results predicted from this numerical study are for simplified 2-D bodies. The comparison of the two sets of results are good enough and this is due to the fact that in drag force estimation the dominant contribution is due to the body section which is of a 2-D nature. Finally, in order to complete this study it was decided to examine the effect of Reynolds number by changing the inlet velocity. Hence for a range of inlet velocities and thus the corresponding Reynold numbers the ratio of the drag coefficients for the Citroen-2CV and the Renault-5 are calculated. The results are shown in Table 2. As it is seen from these results there are only minor changes between the calculated drag ratios. Therefore, it can be concluded that the effect of the Reynolds number is

TABLE 2. Effect of Reynolds Number.

Reynolds Number	Drag Ratio
5000	1.08817
10000	1.07178
30000	1.08368
50000	1.08397
60000	1.08638
75000	1.07952
100000	1.07502

not so crucial.

CONCLUSION

In this paper the flows around a number of car geometries were studied. For this purpose the 2-D incompressible Navier-Stokes equations with a suitable K-ε turbulance model were used. The predicted results are in good agreement with the existing experimental results.

ACKNOWLEDGMENTS

The author expresses his thanks to the research committee members of Isfahan University of Technology for their support to conduct this study.

NOMENCLATURE

English letters

a_i	Amplification factor
b_j	Amplification factor
c_i	Decay factor
c_1, c_2, c_μ	Turbulence constants
d_j	Decay factor
D_x, D_y	Defined parameters
f_1, f_2, f_μ	Turbulence factors
f_x, f_y	Friction force
J	Jacobian
K	Turbulence length
L_{ref}	Reference length
p	Pressure
$p(\xi, \eta)$	Exponential weighting function
$q(\xi, \eta)$	Exponential weighting function
R	Turbulence Reynolds number
Re_∞	Freestream Reynolds number
t	time
u_∞	Freestream Velocity
u, v	Velocity components
x, y	Cartezian space coordinates
x_ξ, x_η, y_ξ, y_η	Transformation metrics

Greek letters

$\alpha, \beta, \gamma, \sigma, \tau$	Transformation parameters
κ	Artificial compressibility factor
ε	Turbulence dissipation
λ	Bulk viscosity coefficient
μ	Dynamic viscosity coefficient
μ_{ref}	Freestream viscosity coefficient
ξ, η	General space coordinates
ρ	Density
ρ_{ref}	Freestream density
σ_k, σ_e	Turbulence coefficients
τ_{xx}, τ_{yy}, τ_{xy}	Normal and shear stresses

REFERENCES

1. Robert. A. Granger, "Fluid Mechanics," Holt-Saunders International Editions, (1985).
2. C. L. Lin, D. W. Pepper and S. C. Lee, "Numerical Methods for Separated Flow Solutions around a Circular Cylinder, *AIAA Journal*, Vol. 14, No. 7, (1976), 900-906.
3. Celika, Patel and Landweber, "Calculation of the Mean Flow Past Circular Cylinders by Viscous-Inviscid Interaction, *Journal of Fluids Engineering*, Vol. 107, (June 1985), 218-223.
4. R. B. Payne, "Calculation of Unsteady Viscous Flow Past a Circular Cylinder, *"Journal of Fluid Mechanics*, Vol. 4, (November 1957), 81-86.
5. S. V. Patankar, "Numerical Heat Transfer and Fluid Flow," (1980).
6. K. A. Hoffmann and S. T. Chiang, "Computational Fluid Dynamics for Engineers," a Publication of Eduction System, Vol. 1, Wichita, Kansas, USA, (1993).
7. V. Michelassi and C. Benocci, "Prediction of Incompressible Flow Separation with Approximate Factorization Technique, *"International Journal for Numerical Methods in Fluids*, Vol. 7, (1987), 1383-1403.
8. A. J. Chorin, "A Numerical Method for Solving

Incompressible Viscous Flow Problem," *Journal of Computational Physics*, Vol. 2, No. 1, (1967), 12-26.

9. W. P. Jones and B. E. Launder, "The Prediction of Laminarization with a Two-Equation Model of Turbulence," *International Journal of Heat and Mass Transfer*, Vol. 35, (1972), 301-314.
10. V. Michelassi and T. H. Shih; "Elliptic Flow Computation by Low Reynolds Number Two-Equation Turbulence Models, " NASA-44135, (1991).
11. J. F. Thompson, F. C. Thamea and C. W. Mastin, "Boundary Fitted Curvilinear Coordinate Systems for Solution of Partial Differential Equations on Fields Containing any Number of Arbitrary Two-Dimensional Bodies," NASA-CR-2729, (1977).